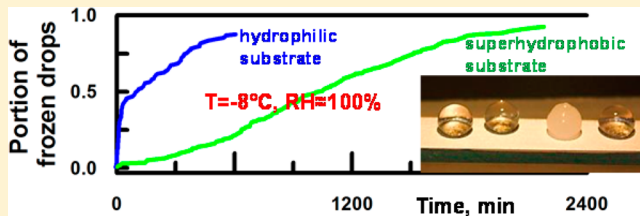


Effect of Wettability on Sessile Drop Freezing: When Superhydrophobicity Stimulates an Extreme Freezing Delay

Ludmila Boinovich,* Alexandre M. Emelyanenko, Vadim V. Korolev, and Andrei S. Pashinin

A. N. Frumkin Institute of Physical Chemistry and Electrochemistry, Russian Academy of Sciences, Leninsky prospect 31, 119071 Moscow, Russia

ABSTRACT: An increasing number of studies directed at supercooling water droplets on surfaces with different wettabilities have appeared in recent years. This activity has been stimulated by the recognition that water supercooling phenomena can be effectively used to develop methods for protecting outdoor equipment and infrastructure elements against icing and snow accretion. In this article, we discuss the nucleation kinetics of supercooled sessile water droplets on hydrophilic, hydrophobic, and superhydrophobic surfaces under isothermal conditions at temperatures of -8 , -10 , and -15 °C and a saturated water vapor atmosphere. The statistics of nucleation events for the ensembles of freezing sessile droplets is completed by the detailed analysis of the contact angle temperature dependence and freezing of individual droplets in a saturated vapor atmosphere. We have demonstrated that the most essential freezing delay is characteristic of the superhydrophobic coating on aluminum, with the texture resistant to contact with ice and water. This delay can reach many hours at $T = -8$ °C and a few minutes at -23 °C. The observed behavior is analyzed on the basis of different nucleation mechanisms. The dissimilarity in the total nucleation rate, detected for two superhydrophobic substrates having the same apparent contact angle of the water drop but different resistivities of surface texture to the contact with water/ice, is associated with the contribution of heterogeneous nucleation on external centers located at the water droplet/air interface.



INTRODUCTION

The supercooling of bulk liquids and the hysteresis of bulk first-order transitions such as freezing have been widely discussed in the literature for several hundred years. For example, the first review of studies of the supercooling phenomenon in water was published in 1775.^{1,2} It is now well established that bulk water freed from external crystallization centers can be supercooled to -41 to -42 °C (i.e., the temperature corresponding to the limiting temperature of homogeneous nucleation^{2–6}). However, an increasing number of experimental and theoretical studies directed particularly at the supercooling of water droplets on surfaces with different wettabilities^{7–17} have appeared in recent years. This activity has been stimulated by the recognition that water supercooling phenomena can be effectively used to develop methods for protecting outdoor equipment and infrastructure elements against icing and snow accretion. Numerous studies have shown that surface wettability affects the nucleation time of supercooled water, and in some cases on superhydrophobic surfaces there is a significant delay before supercooled water freezes.^{10,13–23} This delay allows water droplets to be removed spontaneously from an inclined superhydrophobic surface before they freeze.

It is worth noting that the main mechanism of liquid supercooling is associated with the existence of an energy barrier to nucleation. The value of this barrier can be determined as the maximum work required to form a nucleus of the crystalline phase in the bulk liquid phase for homogeneous nucleation or at the interface between the bulk liquid phase and the external phase for heterogeneous

nucleation. The energy barrier for heterogeneous nucleation may be much lower than for homogeneous nucleation, which in turn decreases the probability of deep supercooling of water droplets on substrates.

Although a number of important findings about the peculiarities of freezing supercooled droplets on surfaces at negative temperatures have been noted in the literature, many peculiarities of freezing water droplets on substrates with various wettabilities still require explanation. The case when water droplets are cooled simultaneously with the substrate and the surrounding environment under homogeneous temperature conditions is of particular interest. In this case, the heat flux between the water and the substrate is minimized. Another important factor that may affect the nucleation of ice is the air humidity and its variation as the air cools. The most important situation for practical applications is when the air humidity is kept close to 100% as the water, surfaces, and air are cooled. Freezing rain and snow disasters actually occur at very high air humidity. As an example, the freezing rain in and around Moscow on December 25–26, 2010 occurred at humidity varying over the range of 94–98%, whereas the average humidity in winter at temperatures from 0 to -20 °C is usually no lower than 75%.

Our aim in this article is to discuss the nucleation times of supercooled water droplets under isothermal conditions. In our

Received: October 1, 2013

Revised: January 23, 2014

Published: January 23, 2014



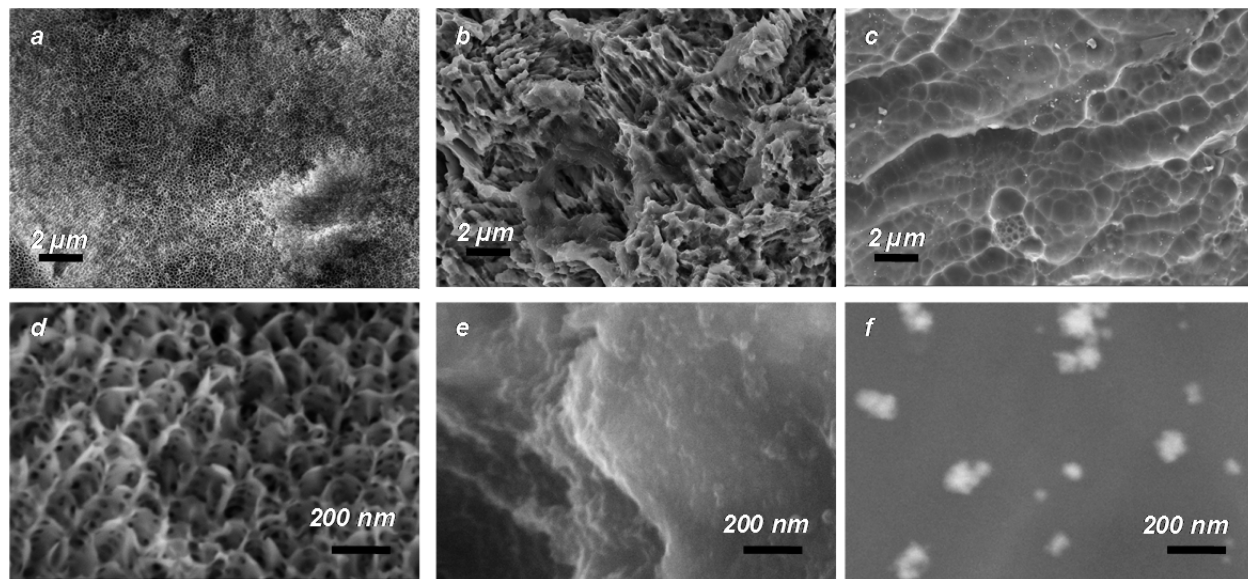


Figure 1. Surface morphologies of the superhydrophobic coating on aluminum (a, d), the superhydrophobic coating on stainless steel (b, e), and hydrophilic/hydrophobic aluminum (c, f). Because the monolayer adsorption of the hydrophobic agent did not change the surface texture, the morphologies of hydrophilic and hydrophobic substrates appeared to be the same. Scale bars are 2 μm (a–c) and 200 nm (d–f).

Table 1. Contact (CA) and Rolling (RA) Angles on Different Samples Used for Experiments with Drops Freezing

state of the coating	sample 1 superhydrophobic coating on aluminum		sample 2 superhydrophobic coating on steel		sample 3 hydrophobic aluminum		sample 4 hydrophilic aluminum	
	CA, deg	RA, deg	CA, deg	RA, deg	CA, deg	RA, deg	CA, deg	RA, deg
freshly prepared coatings	167.5 \pm 2.6	7.6 \pm 3.3	167.5 \pm 3.8	9.6 \pm 2.9	126.5 \pm 1.7		22.3 \pm 3.9	
after eight cycles of freezing/thawing of sessile water drops	166.3 \pm 2.4	12.5 \pm 3.0	165.5 \pm 3.1	15.4 \pm 3.6	106.1 \pm 2.5		35.4 \pm 6.4	

experiments, water droplets deposited on hydrophilic, hydrophobic, or superhydrophobic surfaces were cooled simultaneously with the substrate and the surrounding environment to the required temperature while the humidity was maintained in the vicinity of 100% during the cooling process.

The statistics of freezing events in ensembles of sessile droplets under isothermal conditions in a saturated atmosphere were compared and completed by a detailed analysis of the freezing of individual droplets in a saturated atmosphere. We studied the freezing delay on substrates with different wettabilities for temperatures from 0 to -30°C . To the best of our knowledge, these issues have not been studied in detail in the literature so far. It will be shown that under the above-mentioned conditions water droplets on superhydrophobic surfaces can remain in the supercooled liquid state for many hours.

MATERIALS AND METHODS

In this article, we studied the freezing delay of water droplets on hydrophilic and hydrophobic aluminum surfaces and on two types of superhydrophobic surfaces in a thermally homogeneous environment. The hydrophilic aluminum plates with typical plate sizes of 80 mm \times 10 mm \times 1 mm were obtained by rolling A0 aluminum alloy wires (>99.0 wt % of Al) using a Stan 200 rolling mill. Preliminary sample treatment included immersion in a 20 wt % aqueous solution of potassium hydroxide for 2 min for degreasing, followed by rinsing with distilled water.

The hydrophobic aluminum substrates were prepared by the hydrophobic treatment of hydrophilic plates obtained as described above. The treatment included immersion into a 2 vol % solution of methoxy-{3-[$(2,2,3,3,4,4,5,5,6,6,7,7,8,8,8$ -pentadecafluoroctyl)oxy]propyl}-silane in dehydrated decane for 2 h, followed by rinsing with ethanol and distilled water and drying in an oven at 130°C for 1 h.

The superhydrophobic coatings were formed on both aluminum and 12X18H10T stainless steel samples. The design of the coating on stainless steel was described in detail earlier²² and included chemical etching in a 50 vol % aqueous solution of FeCl_3 and depositing nanoparticles from a wetting film of a dispersion containing silica nanoparticles, the hydrophobic agent methoxy-{3-[$(2,2,3,3,4,4,5,5,6,6,7,7,8,8,8$ -pentadecafluoroctyl)oxy]propyl}-silane, and dehydrated decane as a dispersion medium. A characteristic feature of this type of coating, which is fabricated using nanoparticles, is the occasional detachment of some particles from the coating when it comes in contact with water or ice. Further migration of these particles through the droplet to the water/air interface leads to the appearance of a very small number of crystallization nuclei at the water/air interface. The influence of these nuclei on the crystallization kinetics will be discussed below.

The preparation of the superhydrophobic coating on aluminum included degreasing the aluminum plates as described above, anodic oxidation in the galvanostatic regime in a phosphoric acid solution, washing with distilled water, drying in an oven at 130°C , and finally chemical adsorption of the hydrophobic agent methoxy-{3-[$(2,2,3,3,4,4,5,5,6,6,7,7,8,8,8$ -pentadecafluoroctyl)oxy]propyl}-silane from solution in dehydrated decane. Heat treatment of the sample in an oven at 140°C in the presence of water vapor after solvent evaporation leads to cross-linking between molecules of the hydrophobic agent.²⁴

The morphologies of all types of surfaces are shown in Figure 1. The microstructure of the samples was studied using a Carl Zeiss Supra 40 VP scanning electron microscope. Micrographs were taken at 5 and 10 kV acceleration voltages using secondary (InLens, SE2) electron detectors. Energy-dispersive X-ray (EDX) analysis was performed using an INCA PentaFETx3 analyzer (Oxford Instruments). To minimize the influence of bulk layers, the composition of the surface layer was analyzed at the grazing angle of the incident beam.

Characterization of the wettability of the coatings was based on contact and rolling angle measurements. We used the method of digital video image processing of sessile droplets. The homemade experimental setup for recording optical images of sessile droplets and software for the subsequent determination of droplet parameters using the Laplace curve fitting routine were described earlier.^{25,26} To characterize the wetting of different coatings, initial contact angles for 10–15 μL droplets were measured on five different surface locations for each sample.

To measure the rolling angle, 10 μL droplets were deposited on the surface. After the initial droplet shape was equilibrated, manipulation with an angular positioner allowed us to change the sample surface tilt in a controllable manner and detect the rolling angle by averaging over five different droplets on the same substrate.

Typical contact angles for all surfaces studied and rolling angles for superhydrophobic coatings are presented in Table 1.

The investigation of sessile droplet freezing on thermoelectrically cooled substrates with different wettabilities in undersaturated^{13,21,23,27,28} and supersaturated^{12,13,20,29,30} vapor atmospheres is well documented. However, little attention has been given to experiments performed under isothermal conditions.³¹ To achieve these conditions in our experiments, the droplet, the vapor, and the substrate were thermally homogeneously cooled to the required temperature over 60–75 min, and then the temperature was kept constant. We started to count the time required to freeze the droplets from the instant the desired temperature was established in the experimental chamber.

Two types of experiments were performed in this study. In the first one, the freezing delay for water droplets deposited on substrates with different wettabilities was studied in a thermally homogeneous environment and vapor saturation close to 100%.

Because nucleation in supercooled water droplets is a stochastic process and the nucleation barrier is extremely sensitive to the characteristics of the droplet surface and water impurities,^{32–34} the temperature and time dependences of liquid droplet freezing must be analyzed on the basis of large ensembles of droplets.³⁵ To elucidate the influence of particles and electrolytes contained in natural water, the experiments were performed with tap water as a test liquid (the electroconductivity of the tap water used in all experiments was 4.1 mS/m). Because the nucleation kinetics is very sensitive to the water purity and the presence of suspended particles, the appropriate vessel was filled with tap water at once, and this water was used for all experiments. In each freezing cycle, 13–20 sessile droplets with a volume of 25 μL were deposited on each substrate positioned inside a thin-wall stainless steel hermetic cell with a transparent poly(methyl methacrylate) cover that is 2 cm thick (Figure 2). The low thermal

conductivity of this cover prevents water from condensing on the inside of the cover in the presence of saturated water vapor. The transparent cover also makes it possible to monitor the phase state of droplets by analyzing the video sequence registered with a BestDVR-405 LightNet video system. Freezing of the droplets was detected by the change in appearance from clear to opaque.

The cell with substrates was placed on an antivibration support inside a Binder MK53 environmental chamber with temperature variations of less than 0.3° (as indicated by the manufacturer). Water vapor saturation inside the cell at temperatures above 0 °C was achieved by pouring a 2 mm water layer on the bottom of the cell. The large water evaporation area maintained 100% humidity inside the cell. After droplet deposition, sealing the cell, and equilibration of the vapor phase in the cell for 30 min, the temperature in the environmental chamber was lowered to the desired value over 15 min. However, the hindered diffusion heat exchange between the environmental chamber and the cell resulted in a substantial delay in reaching the equilibrium temperature inside the cell. The temperature of the vapor in the vicinity of the substrates was measured by a Check Temp thermocouple located just under the sample holder. Achieving the desired negative temperature in the cell typically required 60–75 min from the beginning of chamber cooling. The time elapsed from that moment to the freezing of a given droplet was recorded as the freezing time delay for that droplet. The temperature was measured with a resolution of 0.1 °C. The droplet freezing delay was studied at the following constant temperature values: -8, -10, and -15 °C and in the regime of instantaneous slow cooling until -30 °C. The low rate of temperature decrease inside the cell prevented significant vapor supersaturation in the cell and condensation of vapor onto the substrates. Most condensation occurred in the water layer on the bottom of the cell.

Preservation of the heterogeneous wetting regime for droplets on the superhydrophobic substrates was evidenced by the shape of the frozen droplet and by the observation of the phenomenon of total internal reflection at the water/air interface, which caused the mirrorlike appearance of the droplet/substrate contact area.

It is worth noting that whereas a freezing delay was observed for sessile droplets, at the same time a thick water layer at the bottom of the cell was already freezing as the cell was cooled to temperatures of 0 to -3 °C. Freezing of the water layer is well documented by a temperature rise measured by a thermocouple immersed in the water. Because of this freezing, the relative humidity inside the cell becomes temperature-dependent because the vapor pressure above supercooled water exceeds the vapor pressure above ice at the same temperature. Figure 3 presents literature data^{36,37} on water vapor pressure above supercooled water and ice for different negative temperatures. According to these data, the relative humidity in the cell deviates

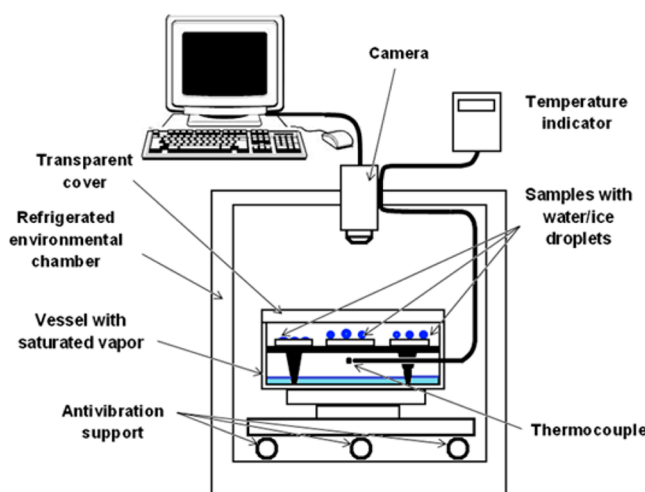


Figure 2. Schematic of the experimental setup for studying the nucleation kinetics.

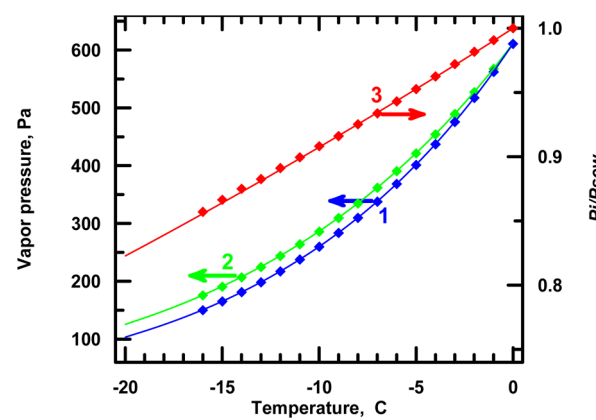


Figure 3. Temperature dependences of saturated vapor pressures above crystallized ice, P_i (1), and supercooled water, P_{scw} (2), and of the relative undersaturation of vapor above the ice with respect to supercooled liquid drops (3). Points are experimental data,³⁶ and lines are calculated using the analytical equations.³⁷

from 100 to 82% at $T = -20^\circ\text{C}$ (Figure 3). At the same time, weak evaporation of a whole ensemble of droplets (containing 36–60 droplets on top of all substrates) leads to a local increase in humidity. As a result, in this type of experiment, the vapor pressure around the droplets approaches the saturated value. Thus, a 25 μL water droplet can be stored in this cell at -15°C for several hours without a noticeable evaporation-induced variation in diameter.

Given the stochastic nature of the nucleation of ice from supercooled water, multiple runs on the same samples were required to determine whether surface wettability and the peculiarities of surface morphology exert a real and statistically significant effect on the freezing delay. The data of the experiments presented below were obtained by an analysis of the freezing of 100 to 200 sessile droplets on each particular substrate at each temperature.

In the second type of experiment, freezing of an individual droplet deposited on the superhydrophobic coating on aluminum was studied in a thermally homogeneous environment at vapor saturation close to 100%. Deionized water (electrical resistance 15 $\text{M}\Omega \text{ m}$) was used as the testing liquid for this type of experiment. The double-walled cell used for these investigations was described earlier.³⁸ We monitored the evolution of water droplet parameters such as the contact angle, base diameter, and apex radius of the water droplet and the liquid surface tension to density ratio as functions of the time of contact of the droplet with the coating during a long-term temperature decrease. To control the temperature and avoid vibrational perturbations of the freezing process, the cell was placed on an antivibration support inside the Binder MK53 environmental chamber.

THEORETICAL BACKGROUND: INFLUENCE OF SUBSTRATE WETTABILITY ON NUCLEATION KINETICS

Classical nucleation theory is usually invoked for a quantitative description of nucleation in liquid water under supercooled conditions.^{39–46} It is assumed that the formation of a single critical nucleus initiates the crystallization of the whole droplet either homogeneously or heterogeneously. This critical nucleus may be associated with a cluster of icelike structures in bulk liquid (homogeneous nucleation) or with an external crystallization center (heterogeneous nucleation), either suspended in the liquid or located at the liquid/air or liquid/substrate interface. The total freezing rate of liquid droplets in an ensemble of monodisperse droplets all containing external crystallization centers of a different nature will be the sum of the rates of homogeneous and heterogeneous nucleation^{39,46}

$$\tilde{J}(T, t) = J^{\text{homo}}(T, t) \cdot v + \sum_i J_i^{\text{hetero}}(T, t) \cdot S_i \quad (1)$$

where J^{homo} is the frequency per unit volume of spontaneous nucleation by the homogeneous mechanism in droplets of volume v , J_i^{hetero} is the frequency per unit surface of spontaneous nucleation by the heterogeneous mechanism on an external nucleus of type i located on wetted surface area S_i , T is the temperature, and t is the time.

For a monodisperse ensemble of droplets with a total population of N_0 and mutually independent freezing events caused by either homogeneous or any type of heterogeneous nucleation, the number of droplets dN_f frozen in time dt can be expressed as

$$dN_f = N(t) \cdot (J^{\text{homo}}(T, t) \cdot v + \sum_i J_i^{\text{hetero}}(T, t) \cdot S_i) dt \quad (2)$$

where $N(t)$ is the total number of unfrozen droplets at time t .

A constant (time-independent) rate of ice nucleation is not immediately established after the water droplet is brought to the supercooled state but after a specific time interval necessary

to create a stationary size distribution of ice embryos.^{39,41–43,47} Thus, the nonstationary rate of nucleation by either the homogeneous or heterogeneous mechanism is expressed by the corresponding values of stationary rates J_α^{st} and time lags τ_α ^{39,47–49}

$$\begin{aligned} J(t) &= \sum_\alpha J_\alpha(t) \cdot A_\alpha \\ &= \sum_\alpha J_\alpha^{\text{st}} \left[1 + 2 \sum_{n=1}^{\infty} (-1)^n \exp\left(\frac{-n^2 t}{\tau_\alpha}\right) \right] \cdot A_\alpha \end{aligned} \quad (3)$$

where $\alpha = \text{homo}, \text{hetero}_1, \text{hetero}_2, \dots, \text{hetero}_k$, $A_{\text{homo}} = v$, and $A_{\text{hetero } i} = S_i$ (area available for heterogeneous nucleation of type i). The series in square brackets is the tabulated function of Kolmogorov's distribution.⁵⁰ The behavior of this function leads to a variation of $J(t)$ values from 0 at $t/\tau_\alpha \rightarrow 0$ to J_α^{st} at $t/\tau_\alpha \rightarrow \infty$.

Integrating eq 2 with the initial condition $N(t = 0) = N_0$ immediately gives the relation between the portion of unfrozen droplets in the population versus time at a particular temperature (isothermal conditions):

$$\log \frac{N(t)}{N_0} = - \sum_i \left\{ J_\alpha^{\text{st}} \cdot A_\alpha \cdot t + 2 J_\alpha^{\text{st}} A_\alpha \tau_\alpha \times \left[\sum_{n=1}^{\infty} \frac{(-1)^{n+1}}{n^2} \exp\left(-n^2 \frac{t}{\tau_\alpha}\right) - \frac{\pi^2}{12} \right] \right\} \quad (4)$$

This equation contains the main experimental parameters in the freezing statistics experiment. Thus, the analysis of experimental data based on eq 4 allows us to estimate the role of different mechanisms of nucleation and the corresponding time lags.

Both the theory and the experiments show that stationary nucleation rates in homogeneous and heterogeneous nucleation are strongly temperature-dependent. This leads to a significant increase in the probability of freezing with decreasing temperature^{39,43,45,46,51–53}

$$J_{\text{homo}}^{\text{st}} = B \cdot T \exp\left(-\frac{E}{k_B T}\right) \exp\left(-\frac{W_{\text{homo}}^*}{k_B T}\right) \quad (5)$$

and

$$J_{i(\text{hetero})}^{\text{st}} = C_i \cdot T \exp\left(-\frac{E_i}{k_B T}\right) \exp\left(-\frac{W_{i(\text{hetero})}^*}{k_B T}\right) \quad (6)$$

where W_{homo}^* and W_{hetero}^* represent the maximum work required to form a nucleus of the crystalline phase in the bulk liquid phase for homogeneous nucleation or at the interface between the bulk liquid phase and the external phase for heterogeneous nucleation, respectively, E and E_i are the diffusion energy for a water molecule to cross the liquid/embryo interface and the activation energy for moving the three-phase contact line, respectively, and B and C_i are constants depending on the characteristic parameters of the liquid and ice nucleus formed on different substrates.

In general, the energy barrier for heterogeneous nucleation W_{hetero}^* may be much lower than for homogeneous nucleation W_{homo}^* .³⁹ For the water/ice phase transition, the relation between the barriers can be written as

$$\begin{aligned} W_{\text{hetero}}^* &= W_{\text{homo}}^* \varphi(\theta) \\ &= W_{\text{homo}}^* \frac{(1 - \cos \theta_{\text{is}(w)})^2}{4} (2 + \cos \theta_{\text{is}(w)}) \end{aligned} \quad (7)$$

where the coefficient $\varphi(\theta)$ is determined by the competitive contact angle $\theta_{\text{is}(w)}$ of substrate (subscript s) wetting by ice (i) in a water environment (w) and reflects the degree of decrease in the nucleation energy barrier on the substrate in comparison to nucleation in bulk water.

As follows from the dependence of the coefficient φ on the corresponding contact angle $\theta_{\text{is}(w)}$ shown in Figure 4 that

$$\lim_{\theta \rightarrow 0} \varphi(\theta) = 0$$

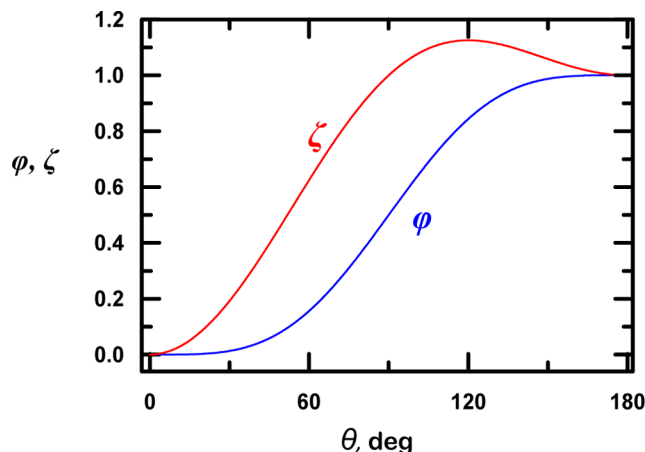


Figure 4. Behavior of functions $\varphi(\theta_{\text{is}(w)})$ and $\zeta(\theta_{\text{is}(w)})$.

In other words, by improving the competitive wetting of the substrate with ice, it is possible to achieve virtually barrier-free formation of ice nuclei on the substrate and thus a zero freezing delay time for water droplets on these substrates. However, the energy barrier for heterogeneous nucleation approaches the barrier characteristic of homogeneous nucleation at $\theta_{\text{is}(w)} \rightarrow 180^\circ$, when the probability of a long-term supercooling state is highest.

Thus, the influence of substrate wettability on the energy barrier to heterogeneous nucleation affects the nucleation kinetics through the stationary rate of heterogeneous nucleation. Another important factor associated with substrate wettability is related to the influence of the wettability of a substrate with water, $\theta_{ws(\text{air})}$, on the value of the water droplet contact diameter on the substrate and hence on the wetted surface area S_i (eq 4). However, on the short time scale of nucleation kinetics, the significant influence of substrate wettability by supercooled water droplets on the time lag must be stressed. As follows from the analysis performed by Toshev and Gutzow,⁴⁷ the time lags τ_α will be different for homogeneous and heterogeneous nucleation. For heterogeneous nucleation, the dependence of time lag τ_{hetero} on the contact angle of comparative wetting of the substrate by ice and water is described by⁴⁷

$$\begin{aligned} \tau_{\text{hetero}} &= \zeta(\theta_{\text{is}(w)}) \cdot \tau_{\text{homo}} \\ &= \left[1 - \frac{\cos \theta_{\text{is}(w)}}{2} - \frac{\cos^2 \theta_{\text{is}(w)}}{2} \right] \tau_{\text{homo}} \end{aligned} \quad (8)$$

The behavior of function $\zeta(\theta_{\text{is}(w)})$ is also shown in Figure 4. Thus, by increasing $\theta_{\text{is}(w)}$ to $\theta_{\text{is}(w)} > 90^\circ$, it is possible to get $\tau_{\text{hetero}} > \tau_{\text{homo}}$, which leads (according to eq 4) to a significant decrease in the heterogeneous nucleation rate in the initial stages of crystallization.

An analysis of eq 4 with a consideration of eqs 5–8 leads to the conclusion that on a long time scale the influence of substrate wettability on the nucleation kinetics is mainly determined by its effect on the energy barrier. On a short time scale for highly hydrophobic surfaces, nonstationary effects characterized by time lags for homogeneous and heterogeneous nucleation play a significant role in the delay in droplet freezing. In addition, an increase in the contact angle of a sessile droplet on the substrate and the transition to a heterogeneous wetting regime diminish the contribution of heterogeneous nucleation at the water/substrate interface to the statistics of freezing events.

RESULTS AND DISCUSSION

Four types of samples were used to investigate nucleation kinetics in an ensemble of sessile droplets. Our aim in this study was to determine the effect of wettability and the role of different types of external crystallization centers on the freezing statistics.

The initial advancing angles are presented in the first row of Table 1, along with the rolling angles for two samples with superhydrophobic coatings. As follows from the experimental data in Table 1, the initial contact angles for the superhydrophobic coatings are similar, and the difference in rolling angles is also insignificant. However, the characteristic difference between these two samples (as mentioned in the Materials and Methods section) is associated with the presence of external crystallization centers at the water/air interface of sessile droplets deposited on the superhydrophobic coating on steel. The source of these centers is the possible detachment of surface-active particles from the coating on steel when it comes into contact with water or ice and their migration through the droplet to the water/air interface.

The statistics of the freezing delay at $T = -15^\circ\text{C}$ for ensembles of tap water droplets deposited on different substrates are shown in Figure 5.

As was mentioned above, time $t = 0$ corresponds to the beginning of the isothermal experiment after establishing isotropic temperature conditions at $T = -15^\circ\text{C}$ in the experimental cell.

An analysis of the data in Figure 5 leads us to conclude that under saturated vapor conditions a sessile water droplet may remain in a metastable supercooled liquid state for more than half an hour, even on a hydrophilic substrate. However, the differences in crystallization delay times on substrates with different wettabilities are obvious, and the number of droplets on superhydrophobic substrates retaining their liquid state at negative temperatures for a long time is substantially larger than for a hydrophilic substrate. At the same time, a large portion of droplets deposited on hydrophilic and hydrophobic substrates were frozen at higher temperatures before establishing the isotropic temperature conditions.

For a more detailed analysis of freezing statistics at $T = -10^\circ\text{C}$, the experimental data are presented in the coordinates of eq 4 (i.e., as $\log(N/N_0) = f(t)$) (Figure 6). As follows from the data of Figure 6, the nucleation kinetics for droplets on substrates with different wettabilities show nonstationary behavior on short time scales, followed by linear dependences

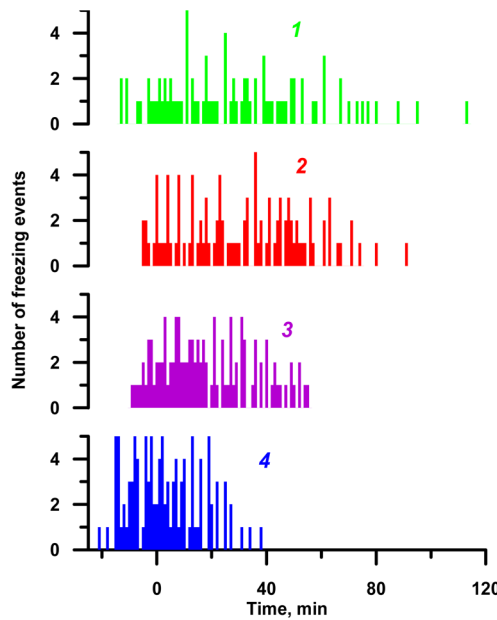


Figure 5. Number of freezing events during 1 min intervals as a function of time elapsed after establishing $T = -15\text{ }^{\circ}\text{C}$ in the experimental cell for $25\text{ }\mu\text{L}$ water droplets on the superhydrophobic coating on aluminum (1), the superhydrophobic coating on stainless steel (2), hydrophobic aluminum (3), and hydrophilic aluminum (4). Negative values of time correspond to droplets that froze before the temperature in the cell reached $-15\text{ }^{\circ}\text{C}$.

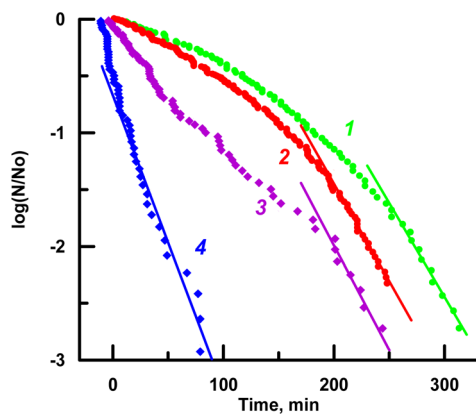


Figure 6. Time dependences of the portion of unfrozen droplets (on a semilogarithmic scale) at $-10\text{ }^{\circ}\text{C}$ for ensembles of $25\text{ }\mu\text{L}$ water droplets on the superhydrophobic coating on aluminum (1), the superhydrophobic coating on stainless steel (2), hydrophobic aluminum (3), and hydrophilic aluminum (4). Lines are linear fits to the long-term part of the nucleation statistics according to eq 9.

characteristic of a time-independent rate of ice nucleation on long time scales. The time lags for nucleation in droplets placed on the substrates used in the investigation increase in the sequence $\tau_{\text{sample } 4} < \tau_{\text{sample } 3} < \tau_{\text{sample } 2} < \tau_{\text{sample } 1}$.

The following conclusions can be derived from eq 8. The crystallization of sessile droplets on short time scales occurs mainly because of heterogeneous nucleation because in homogeneous nucleation the time lags characteristic of different substrates should be the same. Because of the prolonged period of reduced nonstationary nucleation rates for droplets on a superhydrophobic coating on aluminum, the freezing delay for the whole population of droplets is highest on this type of

substrate. As follows from eq 4, the stationary nucleation rates can be defined as

$$\left. \frac{d \ln \frac{N(t)}{N_0}}{dt} \right|_{t \rightarrow \infty} = -\{J_{\text{homo}}^{\text{st}} \cdot v + \sum J_{\text{ihetero}}^{\text{st}} \cdot S_i\} = K \quad (9)$$

The values of parameter K , defined as the slope of the linear portion of the curve for nucleation kinetics on different substrates, are presented in Table 2. Similar values of $K_T = -10\text{ }^{\circ}\text{C}$

Table 2. Rates of Nucleation in Stationary Stages of Freezing Kinetics

sample	K	
	$T = -10\text{ }^{\circ}\text{C}$	$T = -8\text{ }^{\circ}\text{C}$
sample 1	1.7×10^2	1.7×10^3
sample 2	1.7×10^2	2.1×10^3
sample 3	1.8×10^2	2.3×10^3
sample 4	2.6×10^2	3.0×10^3

for the population of droplets on two different superhydrophobic substrates indicate that the leading mechanism of nucleation for these samples is heterogeneous nucleation on dust particles suspended in tap water. The contribution of heterogeneous nucleation on external centers located at the substrate/droplet interface for hydrophilic and hydrophobic substrates differs by 25% from the total stationary nucleation rate for droplets on a hydrophilic surface. This contribution is proportional to the wetted area (see eq 4), which is greater for a hydrophilic substrate. Hence, we may expect a negligible contribution from this type of heterogeneous nucleation for droplets on superhydrophobic substrates, having a much smaller wetted area.

At $T = -8\text{ }^{\circ}\text{C}$, the freezing delay for sessile droplets is much longer than at $T = -15$ and $-10\text{ }^{\circ}\text{C}$, indicating the strong temperature dependence of the nucleation rate, in good agreement with literature data.^{39,43,45,46,51–54} The long-term part of the nucleation statistics (Figure 7) is well fitted by the linear dependences for all substrates. The slopes of the corresponding linear portions of the curves are presented in Table 2.

To analyze the values obtained, we consider the parameters of the liquid droplet/substrate contact. The wetted area of a superhydrophobic substrate under similar water droplets with fixed volume should be equal to $S_i = \pi R^2 f \cdot r$, where R , f , and r are the droplet contact radius, the portion of the wetted area, and the roughness coefficient of the wetted area, respectively. Because the two superhydrophobic substrates studied here were fabricated using the same hydrophobic agent, they may be expected to have Young contact angles close to each other. Then, according to the Cassie–Baxter equation,

$$\cos \theta_{\text{CB}} = \cos \theta_Y \cdot f \cdot r + f - 1 \quad (10)$$

The wetted areas S_i for both superhydrophobic substrates having similar Cassie–Baxter contact angles θ_{CB} , rolling angles (Table 1), and equivalent drop volumes are very likely to be similar or very close to each other. Under such experimental conditions, the difference between values of parameter K (at $T = -8\text{ }^{\circ}\text{C}$; Table 2, third column) characterizing the nucleation statistics on two superhydrophobic substrates can be attributed only to the contribution of heterogeneous nucleation on surface-active nanoparticles located at the water drop/air

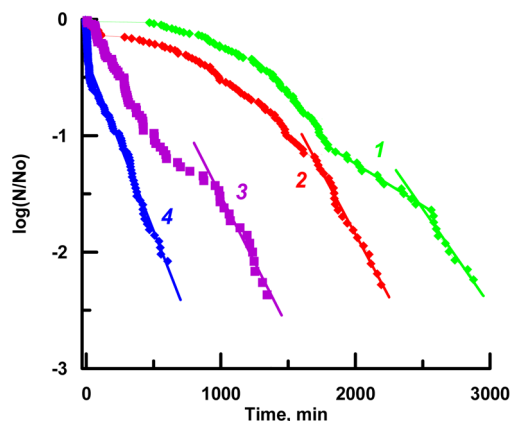


Figure 7. Time dependences of the portion of unfrozen droplets (on a semilogarithmic scale) at $-8\text{ }^{\circ}\text{C}$ for ensembles of $25\text{ }\mu\text{L}$ water droplets on the superhydrophobic coating on aluminum (1), the superhydrophobic coating on stainless steel (2), hydrophobic aluminum (3), and hydrophilic aluminum (4). Lines are linear fits to the long-term part of the nucleation statistics according to eq 9.

interface. As mentioned above, such nucleation centers are present on the surfaces of drops, deposited on sample 2 (the superhydrophobic coating on steel). The comparison of corresponding values indicates the essential contribution of surface-active particles as nucleation centers to the freezing statistics at $T = -8\text{ }^{\circ}\text{C}$.

The total stationary nucleation rate for droplets on substrates with different wettabilities decreases in the order hydrophilic > hydrophobic > superhydrophobic coating on aluminum, with the rate for the hydrophilic substrate (sample 4) being almost twice that for the superhydrophobic substrate. According to the wettability data (Table 1) for drops with equal volumes, the contact area is the largest for the hydrophilic surface,

intermediate for the hydrophobic surface with the same roughness, and smallest for the superhydrophobic substrate as a result of the heterogeneous wetting regime. Thus, the dissimilarity that we detected is associated with the contribution of heterogeneous nucleation on external centers located at the substrate/droplet interface and is related to both the significant difference in the wetted area under a sessile droplet and the variation of W_{hetero}^{*} at different values of $\theta_{\text{is(w)}}$ on substrates with different wettabilities.

In the initial stage of nucleation kinetics, the curves for all substrates show several time segments with transient behavior indicating the significant variation in time lags characteristic of different nucleation mechanisms. According to the literature data (e.g., Bottomley⁵⁵), the contribution of homogeneous nucleation in water at $T = -8\text{ }^{\circ}\text{C}$ may be neglected in comparison to heterogeneous mechanisms. Thus, two different mechanisms of heterogeneous nucleation completing each other are responsible for the nucleation kinetics on all substrates studied. These are nucleation on external crystallization centers either suspended in the liquid or located at the liquid/substrate interface. An additional mechanism of nucleation on surface-active nanoparticles located at the water droplet/air interface is included for the nucleation kinetics in a population of sessile droplets deposited on the superhydrophobic coating on steel.

The analysis presented above was based on the assumption that substrate wettability and the parameters of droplet/substrate contact are weakly dependent on supercooling. However, this point requires more detailed analysis, for which we have performed freezing experiments with individual droplets.

The evolution of the water contact angle on substrates with different wettabilities as the temperature varies from positive to moderately negative values is crucial to understanding the anti-

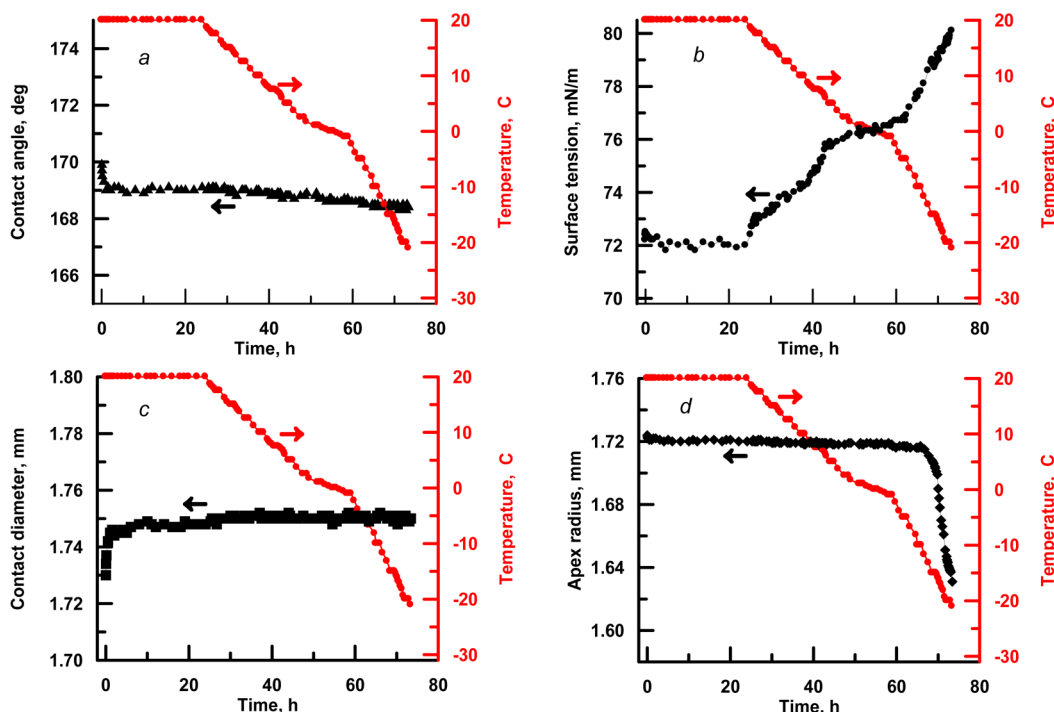


Figure 8. Evolution of experimental drop parameters as a function of the time of exposure to a saturated vapor atmosphere at varying temperature. For these experiments, an individual droplet of deionized water was deposited on the superhydrophobic coating on aluminum (sample 1).

icing performance of various coatings. Some data were obtained under undersaturated and supersaturated conditions for a limited negative temperature interval.^{27,55–58} In these papers, a decrease in the contact angle was detected as the temperature was reduced. In contrast, in a carefully organized experiment³¹ under high humidity (with relative humidity of RH > 80%), the superhydrophobic coatings showed nearly constant values of contact and rolling angles as the temperature was reduced from 20 to –3 °C. In this article, we have studied the evolution of sessile droplet parameters under nearly saturated vapor conditions and a very slow temperature decrease. As an example, Figure 8 presents experimental data on the contact angle (Figure 8a), the ratio of water surface tension to density (Figure 8b), the contact diameter (Figure 8c), and the apex radius (Figure 8d) for a particular droplet as a function of the time of exposure in a saturated vapor atmosphere at varying temperatures.

The regime of temperature reduction is shown on each graph. The behavior shown in Figure 8 is typical, and the difference from sample to sample was associated with the final freezing temperature. The highest freezing temperature for an individual droplet detected in our experiment was –16 °C, and the lowest was –30 °C during exposure to negative temperatures from 12 to 19 h.

As follows from the data of Figure 8a,c, the droplet parameters vary significantly during the first 24 h of exposure in a saturated atmosphere because of the equilibration of the system, as was mentioned earlier.^{24,38} However, a decrease in temperature to –12 °C is accompanied by a decrease in the contact angle in the range of 1° at constant values of the droplet apex radius and contact diameter. For the temperature interval from –12 to –20 °C, a very slight additional decrease in the contact angle is accompanied by a 4% reduction of the apex radius. This decrease is associated with the transition from advancing to receding contact angle due to the reduction of the relative humidity in the experimental cell. (See the discussion of Figure 3.) Thus, an analysis of wettability for high water droplet supercooling indicates the resistance of the superhydrophobic state to negative temperatures and saturated vapor conditions. The increase in the ratio of the water surface tension to density with decreasing temperature correlates well with the literature data.⁵⁹

CONCLUSIONS

The efficiency of the application of superhydrophobic coatings to mitigate an icing problem is determined by a combination of many factors.¹⁷ Thus, important roles for this application include the mechanical and chemical resistance of coatings and the adhesion of ice to such coatings. As shown in the literature, under certain icing conditions the superhydrophobic coatings may fail to demonstrate anti-icing performance.^{60–62} For example, under particular experimental conditions,^{60,62} the adhesion of ice to superhydrophobic surfaces may become stronger than to smooth hydrophobic surfaces. However, in this work we have mainly focused on studying the influence of surface wettability on freezing statistics and revealing different mechanisms of nucleation.

It was shown that at the negative temperatures studied here, in saturated vapor and under thermally homogeneous conditions, the crystallization of sessile water droplets is delayed on all types of substrates from hydrophilic to superhydrophobic. The observed behavior is analyzed on the basis of different nucleation mechanisms.

The longest freezing delay is shown by the superhydrophobic coating on aluminum, characterized by a contact angle of 167.5°, a rolling angle of less than 10°, and high texture resistance to the contact with water. This delay can reach many hours at $T = -8$ °C and a few minutes at –23 °C. The main tendency observed here, which indicates that the increase in time before the start of droplet crystallization is greatest on superhydrophobic substrates compared to hydrophilic substrates, correlates well with the literature data.^{13–19,63} However, in contrast to the above-mentioned studies, our study has shown that the freezing delay time under isothermal conditions in a saturated vapor atmosphere may be many hours, not minutes, as is typical of droplet cooling under nonisothermal conditions. It should be emphasized that, although a conclusion on the slowing of drop crystallization on substrates is noted by all researchers who perform studies in this field, doubts were raised^{12,56,61} that the delay in crystallization on superhydrophobic surfaces is more significant than that in the case of hydrophilic substrates. Some authors⁵⁶ observed no correlation between surface wettability and ice formation, whereas others^{12,61} concluded that the crystallization delay times on hydrophilic substrates exceeded the corresponding values on superhydrophobic surfaces. Such an inconsistency between the above-mentioned results^{12,56,61} and data presented here may be related to two important features of the experiment that were not discussed in the above-mentioned papers. The first is the humidity in the experimental chambers, which differed from 100% in the above-mentioned studies. As was shown by Fuchs,⁶⁴ a drop in an undersaturated atmosphere would have a lower temperature than the ambient vapor phase because of the evaporation of the liquid. However, the supersaturation of the atmosphere results in condensation onto the drop surface and its heating. The deviation of temperature from that in the vapor phase depends on the relative humidity, the drop surface area, and heat exchange between the drop and substrate, and it can reach tens of degrees,⁶⁴ leading to either an inhibition or acceleration of freezing. The second, very important, feature of the experiment is related to the stability of the surface texture in contact with water. Insufficient stability results in the detachment of surface texture elements in contact with a drop and the migration of these particles/texture elements through the droplet to the water/air interface. This phenomenon was observed in our experiments on many superhydrophobic surfaces fabricated with the use of nanoparticles and nanotubes as texture elements. The significant role of the latter feature of superhydrophobic surfaces in the statistics of freezing is considered in this study. The dissimilarity in the total nucleation rate detected for two superhydrophobic substrates with the same apparent contact angle of water droplets but having different surface texture resistances is attributed to the contribution of heterogeneous nucleation on external centers located at the water droplet/air interface.

The difference in nucleation kinetics for the population of droplets on the superhydrophobic (resistant to particle detachment) and hydrophilic/hydrophobic substrates is related to the significant difference in (1) the wetted area under a sessile droplet on these substrates, (2) the energy barriers to heterogeneous nucleation at the substrate/water interface, and (3) nucleation time lags due to different values of the contact angles $\theta_{ws(air)}$ and competitive ice/water wetting $\theta_{is(w)}$.

AUTHOR INFORMATION

Notes

The authors declare no competing financial interest.

ACKNOWLEDGMENTS

This study was financially supported by the Programs for fundamental studies of Presidium of the Russian Academy of Sciences “Fundamental bases of technologies of nanostructures and nanomaterials”, and by a grant for the support of leading scientific schools of the Russian Federation (Project NSh-2181.2014.3).

REFERENCES

- (1) Black, J. The Supposed Effect of Boiling upon Water, in Disposing It to Freeze More Readily, Ascertained by Experiments. *Philos. Trans.* **1775**, *65*, 124–128.
- (2) Angell, C. A. Supercooled Water. *Annu. Rev. Phys. Chem.* **1983**, *34*, 593–630.
- (3) Wilson, P. W.; Heneghan, A. F.; Haymet, A. D. J. Ice Nucleation in Nature: Supercooling Point (SCP) Measurements and the Role of Heterogeneous Nucleation. *Cryobiology* **2003**, *46*, 88–98.
- (4) Zachariassen, K. E.; Kristiansen, E.; Pedersen, S. A.; Hammel, H. T. Ice Nucleation in Solutions and Freeze-Avoiding Insects—Homogeneous or Heterogeneous? *Cryobiology* **2004**, *48*, 309–321.
- (5) Malenkov, G. Liquid Water and Ices: Understanding the Structure and Physical Properties. Topical Review. *J. Phys.: Condens. Matter* **2009**, *21*, 283101.
- (6) Trinh, E.; Apfel, R. E. Sound Velocity of Supercooled Water down to –33 °C Using Acoustic Levitation. *J. Chem. Phys.* **1980**, *72*, 6731–6735.
- (7) Ruan, M.; Li, W.; Wang, B. S.; Deng, B. W.; Ma, F. M.; Yu, Z. L. Preparation and Anti-Icing Behavior of Superhydrophobic Surfaces on Aluminum Alloy Substrates. *Langmuir* **2013**, *29*, 8482–8491.
- (8) Suzuki, S.; Nakajima, A.; Yoshida, N.; Sakai, M.; Hashimoto, A.; Kamemoto, Y.; Okada, K. Hydrophobicity and Freezing of a Water Droplet on Fluoroalkylsilane Coatings with Different Roughnesses. *Langmuir* **2007**, *23*, 8674–8677.
- (9) Jung, S.; Tiwari, M. K.; Doan, N. V.; Poulikakos, D. Mechanism of Supercooled Droplet Freezing on Surfaces. *Nat. Commun.* **2012**, *3*, 615.
- (10) Sarshar, M. A.; Swarctz, C.; Hunter, S.; Simpson, J.; Choi, C.-H. Effects of Contact Angle Hysteresis on Ice Adhesion and Growth on Superhydrophobic Surfaces under Dynamic Flow Conditions. *Colloid Polym. Sci.* **2013**, *291*, 427–435.
- (11) Tourkine, P.; Le Merrer, M.; Quere, D. Delayed Freezing on Water Repellent Materials. *Langmuir* **2009**, *25*, 7214–7216.
- (12) Li, K.; Xu, S.; Shi, W.; He, M.; Li, H.; Li, S.; Zhou, X.; Wang, J.; Song, Y. Investigating the Effects of Solid Surfaces on Ice Nucleation. *Langmuir* **2012**, *28*, 10749–10754.
- (13) Alizadeh, A.; Yamada, M.; Li, R.; Shang, W.; Otta, S.; Zhong, S.; Ge, L.; Dhinojwala, A.; Conway, K. R.; Bahadur, V.; Vinciguerra, A. J.; Stephens, B.; Blohm, M. L. Dynamics of Ice Nucleation on Water Repellent Surfaces. *Langmuir* **2012**, *28*, 3180–3186.
- (14) Wang, H.; He, G.; Tian, Q. Effects of Nano-Fluorocarbon Coating on Icing. *Appl. Surf. Sci.* **2012**, *258*, 7219–7224.
- (15) Boreyko, J. B.; Collier, C. P. Delayed Frost Growth on Jumping-Drop Superhydrophobic Surfaces. *ACS Nano* **2013**, *7*, 1618–1627.
- (16) Hejazi, V.; Sobolev, K.; Nosonovsky, M. From Superhydrophobicity to Icephobicity: Forces and Interaction Analysis. *Sci. Rep.* **2013**, *3*, 2194.
- (17) Boinovich, L. B.; Emelyanenko, A. M. Anti-Icing Potential of Superhydrophobic Coatings. *Mendeleev Commun.* **2013**, *23*, 3–10.
- (18) Momen, G.; Farzaneh, M.; Jafari, R. Wettability Behaviour of RTV Silicone Rubber Coated on Nanostructured Aluminum Surface. *Appl. Surf. Sci.* **2011**, *257*, 6489–6493.
- (19) Arianpour, F.; Farzaneh, M.; Kulichin, S. A. Hydrophobic and Ice-Retarding Properties of Doped Silicone Rubber Coatings. *Appl. Surf. Sci.* **2013**, *265*, 546–552.
- (20) Rykaczewski, K.; Anand, S.; Subramanyam, S. B.; Varanasi, K. K. Mechanism of Frost Formation on Lubricant-Impregnated Surfaces. *Langmuir* **2013**, *29*, 5230–5238.
- (21) Huang, L.; Liu, Z.; Liu, Y.; Gou, Y.; Wang, L. Effect of Contact Angle on Water Droplet Freezing Process on a Cold Flat Surface. *Exp. Therm. Fluid Sci.* **2012**, *40*, 74–80.
- (22) Boinovich, L. B.; Emelyanenko, A. M.; Ivanov, V. K.; Pashinin, A. S. Durable Icephobic Coating for Stainless Steel. *ACS Appl. Mater. Interfaces* **2013**, *5*, 2549–2554.
- (23) Zhang, Y. F.; Yu, X. Q.; Wu, H.; Wu, J. Facile Fabrication of Superhydrophobic Nanostructures on Aluminum Foils with Controlled-Condensation and Delayed-Icing Effects. *Appl. Surf. Sci.* **2012**, *258*, 8253–8257.
- (24) Boinovich, L.; Emelyanenko, A. A Wetting Experiment as a Tool to Study the Physicochemical Processes Accompanying the Contact of Hydrophobic and Superhydrophobic Materials with Aqueous Media. *Adv. Colloid Interface Sci.* **2012**, *179*, 133–141.
- (25) Emelyanenko, A. M.; Boinovich, L. B. Application of Dynamic Thresholding of Video Images for Measuring the Interfacial Tension of Liquids and Contact Angles. *Instrum. Exp. Tech.* **2002**, *45*, 44–49.
- (26) Emelyanenko, A. M.; Boinovich, L. B. The Use of Digital Processing of Video Images for Determining Parameters of Sessile and Pendant Droplets. *Colloid J.* **2001**, *63*, 159–172.
- (27) Karmouch, R.; Ross, G. G. Experimental Study on the Evolution of Contact Angles with Temperature near the Freezing Point. *J. Phys. Chem. C* **2010**, *114*, 4063–4066.
- (28) Farhadi, S.; Farzaneh, M.; Kulichin, S. A. Anti-Icing Performance of Superhydrophobic Surfaces. *Appl. Surf. Sci.* **2011**, *257*, 6264–6269.
- (29) Furuta, T.; Sakai, M.; Isobe, T.; Nakajima, A. Effect of Dew Condensation on the Wettability of Rough Hydrophobic Surfaces Coated with Two Different Silanes. *Langmuir* **2010**, *26*, 13305–13309.
- (30) Zhang, Q.; He, M.; Zeng, X.; Li, K.; Cui, D.; Chen, J.; Wang, J.; Song, Y.; Jiang, L. Condensation Mode Determines the Freezing of Condensed Water on Solid Surfaces. *Soft Matter* **2012**, *8*, 8285–8288.
- (31) Yeong, Y. H.; Steele, A.; Loth, E.; Bayer, I.; De Combarieu, G.; Lakeman, C. Temperature and Humidity Effects on Superhydrophobicity of Nanocomposite Coatings. *Appl. Phys. Lett.* **2012**, *100*, 053112.
- (32) Sear, R. P. Estimation of the Scaling of the Nucleation Time with Volume When the Nucleation Rate Does Not Exist. *Cryst. Growth Des.* **2013**, *13*, 1329–1333.
- (33) Hedges, L. O.; Whitelam, S. Patterning a Surface So As to Speed Nucleation from Solution. *Soft Matter* **2012**, *8*, 8624–8635.
- (34) Holbrough, J. L.; Campbell, J. M.; Meldrum, F. C.; Christenson, H. K. Topographical Control of Crystal Nucleation. *Cryst. Growth Des.* **2012**, *12*, 750–755.
- (35) Vali, G. Repeatability and Randomness in Heterogeneous Freezing Nucleation. *Atmos. Chem. Phys.* **2008**, *8*, 5017–5031.
- (36) Spravochnik Khimika (Chemist's Handbook); Nikolsky, B. P., Ed.; Goskhimizdat: Leningrad, 1962; Vol. 1.
- (37) Murphy, D. M.; Koop, T. Review of the Vapour Pressures of Ice and Supercooled Water for Atmospheric Applications. *Q. J. R. Meteorol. Soc.* **2005**, *131*, 1539–1565.
- (38) Boinovich, L.; Emelyanenko, A. M.; Pashinin, A. S. Analysis of Long-Term Durability of Superhydrophobic Properties under Continuous Contact with Water. *ACS Appl. Mater. Interfaces* **2010**, *2*, 1754–1758.
- (39) Skripov, V. P.; Koverda, V. P. Spontannaya Kristallizatsiya Pereokhlazhdennykh Zhidkostey (Spontaneous Crystallization of Supercooled Liquids), Nauka: Moscow, 1984 (in Russian).
- (40) Volmer, M. Kinetik der Phasenbildung; Steinkopf: Dresden, Germany, 1939.
- (41) Frenkel, J. Kinetic Theory of Liquids; Dover: New York, 1955.
- (42) Zeldovich, Ya. B. Zhurn. Eksp. Teor. Fiz. **1942**, *12*, 525 (in Russian).
- (43) Pruppacher, H. R.; Klett, J. D. Microphysics of Clouds and Precipitation; Kluwer: Dordrecht, The Netherlands, 1997.

- (44) Duft, D.; Leisner, T. Laboratory Evidence for Volume-Dominated Nucleation of Ice in Supercooled Water Microdroplets. *Atmos. Chem. Phys.* **2004**, *4*, 1997–2000.
- (45) Marcolli, C.; Gedamke, S.; Peter, T.; Zobrist, B. Efficiency of Immersion Mode Ice Nucleation on Surrogates of Mineral Dust. *Atmos. Chem. Phys.* **2007**, *7*, 5081–5091.
- (46) Murray, B. J.; Broadley, S. L.; Wilson, T. W.; Atkinson, J. D.; Wills, R. H. Heterogeneous Freezing of Water Droplets Containing Kaolinite Particles. *Atmos. Chem. Phys.* **2011**, *11*, 4191–4207.
- (47) Toschev, S.; Gutzow, I. Time Lag in Heterogeneous Nucleation due to Nonstationary Effects. *Phys. Status Solidi* **1967**, *21*, 683–691.
- (48) Collins, F. C. Time Lag in Spontaneous Nucleation Due to Non-Steady Effects. *Z. Elektrochem.* **1955**, *59*, 404–407.
- (49) Kashchiev, D. Solution of Non-Steady State Problem in Nucleation Kinetics. *Surf. Sci.* **1969**, *14*, 209–220.
- (50) Bolshev, L. N.; Smirnov, N. V. *Tablitsy Matematicheskoi Statistiki (Tables of Mathematical Statistics)*; Nauka: Moscow, 1965 (in Russian).
- (51) Fokin, V. M.; Yuritsyn, N. S.; Zanotto, E. D.; Jurn W.P. Schmelzer, J. W. P.; Cabral, A. A. Nucleation Time-Lag from Nucleation and Growth Experiments in Deeply Undercooled Glass-Forming Liquids. *J. Non-Cryst. Solids* **2008**, *354*, 3785–3792.
- (52) Stockel, P.; Ingelheim, B.; Weidinger, I. M.; Baumgartel, H.; Leisner, T. Rates of Homogeneous Ice Nucleation in Levitated H₂O and D₂O Droplets. *J. Phys. Chem. A* **2005**, *109*, 2540–2546.
- (53) Murray, B. J.; Broadley, S.; Wilson, T. W.; Bull, S.; Wills, R. Kinetics of the Homogeneous Freezing of Water. *Phys. Chem. Chem. Phys.* **2010**, *12*, 10380–10387.
- (54) Piucco, R. O.; Hermes, C. J. L.; Melo, C.; Barbosa, J. R., Jr. A Study of Frost Nucleation on Flat Surfaces. *Exp. Thermal Fluid Sci.* **2008**, *32*, 1710–1715.
- (55) Bottomley, G. A. The Vapour Pressure of Supercooled Water and Heavy Water. *Aust. J. Chem.* **1978**, *31*, 1177–1180.
- (56) Yin, L.; Xia, Q.; Xue, J.; Yang, S.; Wang, Q.; Chen, Q. In Situ Investigation of Ice Formation on Surfaces with Representative Wettability. *Appl. Surf. Sci.* **2010**, *256*, 6764–6769.
- (57) Muckenaupt, B.; Ensikat, H.-J.; Spaeth, M.; Barthlott, W. Superhydrophobicity of Biological and Technical Surfaces under Moisture Condensation: Stability in Relation to Surface Structure. *Langmuir* **2008**, *24*, 13591–13597.
- (58) He, M.; Li, H.; Wang, J.; Song, Y. Superhydrophobic Surface at Low Surface Temperature. *Appl. Phys. Lett.* **2011**, *98*, 093118.
- (59) Holten, V.; Bertrand, C. E.; Anisimov, M. A.; Sengers, J. V. Thermodynamics of Supercooled Water. *J. Chem. Phys.* **2012**, *136*, 094507.
- (60) Kulinich, S. A.; Farhadi, S.; Nose, K.; Du, X. W. Superhydrophobic Surfaces: Are They Really Ice-Repellent? *Langmuir* **2011**, *27*, 25–29.
- (61) Jung, S.; Dorrestijn, M.; Raps, D.; Das, A.; Megaridis, C. M.; Poulikakos, D. Are Superhydrophobic Surfaces Best for Icephobicity? *Langmuir* **2011**, *27*, 3059–3066.
- (62) Chen, J.; Liu, J.; He, M.; Li, K. Y.; Cui, D. P.; Zhang, Q. L.; Zeng, X. P.; Zhang, Y. F.; Wang, J. J.; Song, Y. L. Superhydrophobic Surfaces Cannot Reduce Ice Adhesion. *Appl. Phys. Lett.* **2012**, *101*, 111603.
- (63) Li, H.; Zhao, Y.; Yuan, X. Facile Preparation of Superhydrophobic Coating by Spraying a Fluorinated Acrylic Random Copolymer Micelle Solution. *Soft Matter* **2013**, *9*, 1005–1009.
- (64) Fuchs, N. A. *Isparenie i Rost Kapel v Gazoobraznoi Srede (Evaporation and Droplet Growth in Gaseous Media)*; Izd. Akad. Nauk SSSR, Moscow, 1958; in Russian, Engl. transl. by Pratt, J. M.; , ed. Bradley, R. S. Pergamon Press: London, 1959.